Available online at www.sciencedirect.com
ScienceDirect
International Journal of Heat and Mass Transfer 50 (2007) 3616–3623
International Journal of HEAT and MASS TRANSFER
www.elsevier.com/locate/ijhmt

# Nonlinear dynamics of directional solidification with a mushy layer. Analytic solutions of the problem

D.V. Alexandrov [a,*], D.L. Aseev [a], I.G. Nizovtseva [a], H.-N. Huang [b], D. Lee [b]

[a] Urals State University, Department of Mathematical Physics, Lenin Avenue 51, Ekaterinburg 620083, Russian Federation
[b] Tunghai University, Department of Mathematics, Box 859, Taichung 407, Taiwan

Received 23 February 2007
Available online 12 April 2007

**Abstract**

We present new analytic results relating to the nonstationary Stefan-type problems for the unidirectional solidification of binary solutions or melts with a mushy layer. Our detailed analysis of the field data is based on the classical model of a mushy layer, which is modified in order to obtain explicit solutions (solid phase thickness and growth rate, temperature distributions, conductive and latent heat fluxes are determined). Predictions for the growth rate and temperature profiles of the mixed-phase and solid regions agree well with existing observations on young sea ice dynamics.


*Keywords:* Solidification; Mushy; Layer; Sea ice

## 1. Introduction

In spite of the extended history of study of solidification, many aspects of the physics of this phenomenon remain unclear. Aspects of forming of various types of micro- and macrostructures in solids obtained by solidification, the physical mechanisms of which remain to a large degree unclear, are of particular importance. Traditionally the study of directional solidification was and is performed within the framework of the classical model [1], leading to the Stefan boundary value problem. In this approach it is assumed that the liquid and solid phases are separated by a clearly expressed smooth (planar, cylindrical, spherical, etc.) interface between the phases, heat transfer occurs by conduction according to the Fourier law and the velocity of the crystallization front is controlled by the absorption of heat by the solid phase. The mathematical formulations corresponding to these physical models belong to the class of highly-nonlinear problems with moving boundaries. Methods of solutions of these problems have been extensively investigated, among others, in Refs. [2–6]. Due to the difficulties in obtaining analytical solutions, a wide range of numerical methods has also been reported by Crank [6] and references therein. In spite of the appreciable progress attained in investigating these problems, it became clear during the past several years that this approach is limited. So, for example, Ivantsov [7] demonstrated that, under certain conditions, a region of impurity-induced supercooling i.e., one in which the temperature is lower than the temperature of the phase transition, forms in the liquid phase. One of the major achievements in this field doubtlessly consists in the possibility that the morphological stability of the crystallization front may be disturbed, a finding established experimentally by Tiller [8,9] and validated analytically by Mullins and Sekerka [10]. However, the scenario suggested by Mullins and Sekerka takes place when the kinetics of formation of elements of the new phase within the supercooled region is frozen. Another scenario of the development of directional solidification of the binary melt or solution was suggested by Borisov [11] (see also Refs. [12,13]). His theory of the quasiequilibrium two-phase (mushy) layer is based on

* Corresponding author. Tel.: +7 343 3 507541; fax: +7 343 3 507401.
*E-mail address:* Dmitri.Alexandrov@usu.ru (D.V. Alexandrov).

0017-9310/$ - see front matter © 2007 Elsevier Ltd. All rights reserved.
doi:10.1016/j.ijheatmasstransfer.2007.02.006

**Nomenclature**

| | |
|---|---|
| $a$ | solid–mushy layer boundary |
| $b$ | mushy layer–liquid boundary |
| $c$ | specific heat capacity |
| $C$ | impurity concentration (brine salinity) |
| $h$ | front position |
| $k$ | thermal conductivity |
| $L_V$ | latent heat of solidification |
| $m$ | liquidus slope |
| $t$ | time |
| $T$ | temperature |
| $z$ | spatial coordinate |

*Greek symbols*

| | |
|---|---|
| $\rho$ | density |
| $\varphi$ | solid phase fraction |

*Subscripts*

| | |
|---|---|
| i | properties of solid (sea ice) |
| w | properties of liquid (water) |
| m | properties of mushy layer |

the assumption that the nascent supercooling is instantaneously reduced by growing dendrites and that there forms some structureless two-phase zone, separating the crystal and melt (this case corresponds in a certain sense to rapid kinetics of formation of elements of the new phase in the metastable zone). The morphological instability of the phase interface and the instability of the metastable constitutionally supercooled binary solution (melt) cause a system of elements of the solid phase in the form of dendrites, columnar and uniaxial crystals to appear in the liquid phase. The development of this system reduces the supercooling and leads to formation of a new stable solidification mode characterized by the presence of a mushy layer that separates the crystal and the solution. The study of relationships governing solidification in the presence of a mushy region is extremely complicated. This happens because it is necessary to investigate the interaction of nonlinear heat and mass transfer, phase transitions at the solid/mush/liquid interfaces, as well as within the solution. This situation stimulated the search of new, unconventional approaches to modeling the solidification with a mushy layer. One of such constructive approaches consists in the following. A relaxation time of the temperature field is essentially less than a relaxation time of the diffusion field. In particular, the latter explains why the temperature field is described by linear profiles (see, among others, field observations carried out by The LeadEx Group [14]). Moreover, diffusion fluxes play an important role frequently only within a mushy layer. If this is really the case, the mass balance equation takes the form of the Scheil equation [15]. Our theory is devoted to the question how to construct analytic solutions describing real solidification processes with a mush on the basis of the aforementioned principles. In particular, in order to compare our theory with experiments, let us pay our attention to modeling the solidification of young sea ices playing a very important role in the surface heat and mass balance of the Arctic Ocean. This ice is formed, for example, due to the divergence of wind stress which continually produces cracks in the perennial sea ice cover known as leads. In the Arctic winter, the relatively warm water in leads is exposed to the cold air above it. A thin veneer of ice rapidly forms across an exposed lead. After one day's growth the layer of ice is about 10 cm deep, which is still thin compared with the surrounding ice, which is typically several metres thick. We consider the initial formation of ice in leads and its growth during the first few days on the basis of observations carried out by Morison and others [14]. A detailed description of the scientific program and observations has been given by Morison et al. [14] and Wettlaufer et al. [16]. We will not dwell on this point in detail. However, we will point out main features of the Lead Experiment field campaign. There were four main lead deployments during the 6-week experiment. A particularly interesting deployment is "lead 3" which was the largest (approximately a kilometer wide) lead. Deployment at lead 3 began early on the morning of April 6, 1992 and was evacuated 2 days later. We describe observations from both of the buoys that were deployed late on the afternoon of April 6, 1992 (buoy 5 was deployed $\sim$2 hours before buoy 6). For the goals of our theory, we briefly outline the frontal model and discuss its predictions about sea ice dynamics. Of course, our subsequent theory is well suited for solidification of melts within the framework of physical hypotheses under consideration.

## 2. Planar front

Let us now demonstrate how one of the simplest models of the planar front works in practice. Let us now analyze a system consisting of a binary melt or solution and a solid phase (e.g. sea water and ice), separated by some interface $z = h(t)$, where $z$ is the spatial coordinate and $\tau$ is the time. The system under consideration is shown in Fig. 1a: solid and liquid phases are divided by the phase transition boundary, $h(t)$, moving downwards in the liquid because the solid wall, $z = 0$, is cooled with time oscillations. The (atmospheric) temperature, $T_{at}(t)$, determined at $z = 0$, will be regarded as experimentally known. Now, we treat the process as fully thermally controlled. On this basis, the heat transfer process is described by the local conservation of heat within the solid

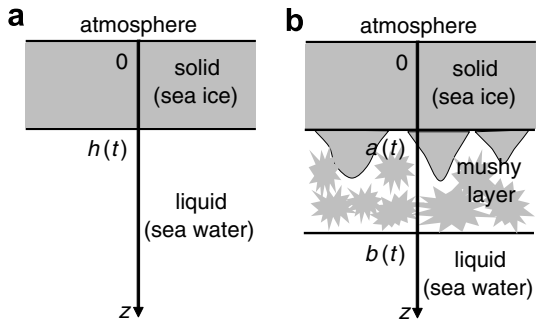


Fig. 1. A scheme illustrating the models with a planar front (a) and mushy layer (b).

$$\frac{\partial T_{\mathrm{i}}}{\partial t} = a_{\mathrm{i}} \frac{\partial^2 T_{\mathrm{i}}}{\partial z^2}, \quad a_{\mathrm{i}} = \frac{k_{\mathrm{i}}}{\rho_{\mathrm{i}} c_{\mathrm{i}}}, \quad 0 < z < h(t) \tag{1}$$

supplemented by the Stefan condition (a heat balance) at the planar interface, which is

$$k_{\mathrm{i}} \frac{\partial T_{\mathrm{i}}}{\partial z} = L_V \frac{\mathrm{d}h}{\mathrm{d}t}, \quad z = h(t), \tag{2}$$

where $L_{\mathrm{V}}$ is the latent heat released as the solid fraction increases, $k_{\mathrm{i}}$ is the thermal conductivity, $\rho_{\mathrm{i}}$ is the density, and $c_{\mathrm{i}}$ is the specific heat capacity of the solid (sea ice). The liquid phase (ocean) is treated as isothermal, which is to say that the temperature field $T_{\mathrm{w}} = \mathrm{const}$ for $z \geqslant h(t)$. Analyzing experimental curves (see Fig. 2), we conclude that the temperature distribution in the young sea ice (solid phase) can be regarded as a nearly linear function of the spatial coordinate $z$. From the physical point of view this means that the temperatures at different depths undergo near-self-similar change (Fig. 2b and d) with small variations from full self-similarity. From the mathematical point of view this means that Eq. (1) takes the form $\partial^2 T_{\mathrm{i}}(z,t)/\partial z^2 = 0$. This is because that the temperature relaxation time is many times less than a characteristic time of the front motion. Taking into account the latter, we arrive at the linear temperature profile within the solid (sea ice)

$$T_{\mathrm{i}}(z,t) = T_{\mathrm{at}}(t) + \frac{T_{\mathrm{w}} - T_{\mathrm{at}}(t)}{h(t)} z. \tag{3}$$

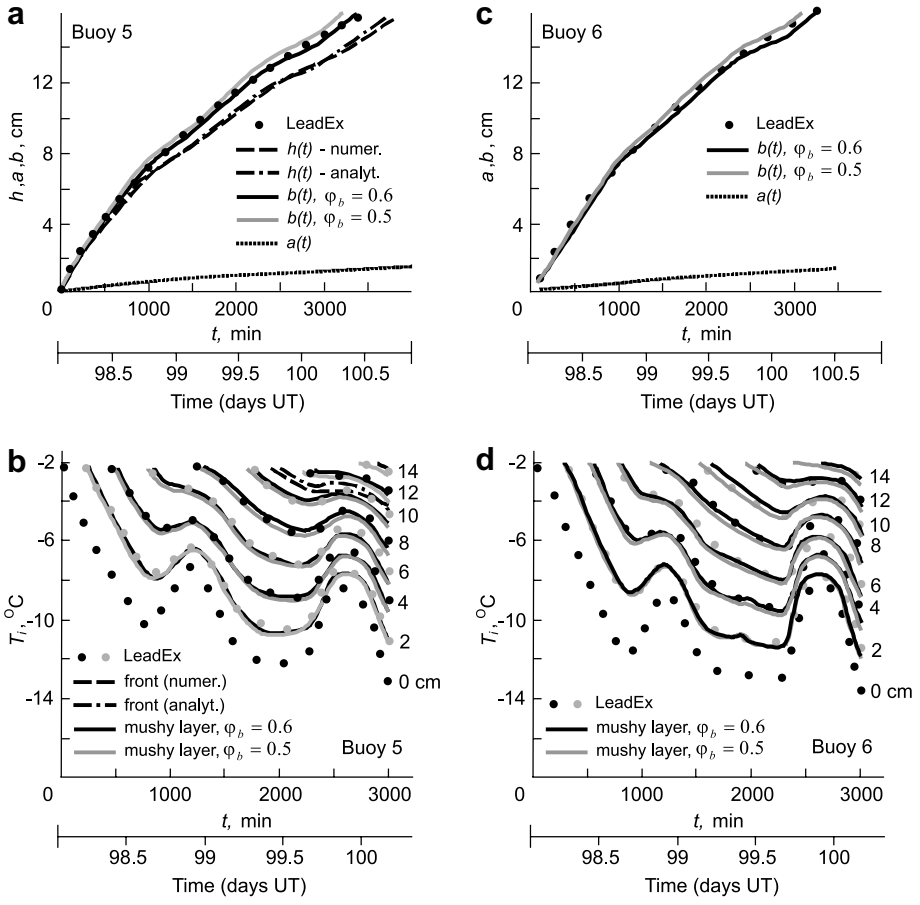


Fig. 2. Time series of ice thickness and temperature–time traces for (a,b) buoy 5 and (c,d) buoy 6 at lead 3 in accordance with the LeadEx experiment and the theory under consideration. The ice–mushy layer boundary is a good approximation to the data for $\varphi_b = 0.5$ and $\varphi_b = 0.6$ (these dependencies are shown by means of function $a(t)$). Numbers at the curves corresponding to each trace designate the depths (expressed in centimeters) measured from the ice/atmosphere interface. The curve at $z = 0$ cm represents the atmospheric temperature ($T_{\mathrm{at}}(t)$) at the ice surface. The time scale used by the LeadEx investigators is decimal days of 1992, abbreviated as UT and denoted on the figure. The time origin in minutes corresponds to 0221, day 98 UT. Physical properties used in calculations: $T_{\mathrm{w}} = -2\ ^{\circ}\mathrm{C}$, $L_V = 3072 \times 10^5\ \mathrm{W\ s\ m^{-3}}$, $k_{\mathrm{i}} = 2.03\ \mathrm{W\ m^{-1}\ ^{\circ}C^{-1}}$, $k_{\mathrm{w}} = 0.56\ \mathrm{W\ m^{-1}\ ^{\circ}C^{-1}}$, $D_{\mathrm{w}} = 1.2 \times 10^{-9}\ \mathrm{m^2\ s^{-1}}$.

The position of the planar solid–liquid interface is found from condition (2). Namely

$$h(t) = \sqrt{\frac{2k_i}{L_V}(T_w t - \int_0^t T_{at}(\alpha)\,d\alpha)}, \quad (4)$$

where the initial condition of the form $h(0) = 0$ is taken into account.

Time series of ice thickness and temperature–time traces in accordance with expressions (3) and (4) are shown in Fig. 2a and b for buoy 5 by the dash-dotted lines. It is easily seen that this frontal solution rather poorly describes experimental data (this line is drawn only for $z = 10$ cm in Fig. 2b). To test the validity of expressions (3) and (4) (instead of the partial differential equation (1) with corresponding boundary conditions) we demonstrate our numerical solution of expressions (1) and (2) by the dashed curves in Fig. 2a and b. One can readily see that the dashed and dash-dotted curves coincide very closely whereas, as before, the curves obtained numerically and experimentally are widely spaced.

Further, if we forget for a minute that the temperature $T_w$ is constant, that is, if we consider it as a free time-dependent parameter, we conclude that an increase in the absolute value of $T_w$ decreases the calculated $h(t)$ for each fixed $t$, i.e. the front positions, obtained from expression (4), move $h(t)$ away from experimental data. On the other hand, the temperature profiles $T_i(z,t)$, obtained from expression (3) for fixed $z$, approach experimental data for this same increase in $|T_w|$. Decreasing the absolute value of $T_w$ leads to the opposite conclusions. It immediately follows that variations in the temperature $T_w$ cannot reconcile theory and observations or, in other words, the frontal theory does not adequately describe experimental data. This is, apparently, due to the fact that the clear dividing boundary "solid–liquid" of the phase transition does not exist in natural conditions. In other words, the phase transition occurs in a layer, filled with the liquid and solid material, which is ahead of the purely sea ice. Such a layer will be considered below. Now, let us emphasize that the linear temperature profile (3) is in good agreement with the frontal model and, perhaps, this profile describes most initial stages of the process.

## 3. Mushy layer

Let us analyze the solidification of a binary mixture with a mushy region, in which heterogeneous inclusions of the new phase (dendrites or crystals) grow in such a manner that this region is virtually totally desupercooled [5,11]. We consider a semi-infinite region ($z > 0$) filled with the solid material ($0 < z < a(t)$), the mushy layer ($a(t) < z < b(t)$), and the liquid phase ($z > b(t)$). Here $a(t)$ and $b(t)$ represent the solid/mushy layer and mushy layer/liquid phase transition boundaries (Fig. 1b). As before, our analysis will be based on the assumption of a linear temperature profile in the solid phase with respect to the spatial coordinate, i.e.

$$T_i(z,t) = T_{at}(t) + C_1(t)z, \quad 0 < z < a(t), \quad (5)$$

where $C_1(t)$ is a time-dependent function. This expression is based on observations given by Morison et al. [14] (see also Wettlaufer and others, [16]) and aforementioned discussions.

By analogy, by reason of self-similarity, the temperature profile within the mushy layer will be considered as a linear function of $z$, i.e.

$$T_m(z,t) = T_1(t) + zT_2(t), \quad a(t) < z < b(t), \quad (6)$$

where time-dependent functions $T_1(t)$ and $T_2(t)$ will be found below (gradients of distributions (5) and (6) are different). From the physical point of view, the temperature linearity means that the ralaxation time of the temperature field is not only less than a characteristic time for growth of the mushy layer, but also less than the time associated with variation in solid fraction in the mushy layer. What is more, the question of why expression (6) approximately satisfies to the classical heat transfer equation

$$\rho_m c_m \frac{\partial T_m}{\partial t} = \frac{\partial}{\partial z}\left[k_m(\varphi)\frac{\partial T_m}{\partial z}\right] + L_V \frac{\partial \varphi}{\partial t} \quad (7)$$

will be discussed below. Here $\rho_m$ is the density, $c_m$ is the heat capacity, and $k_m$ is the conductivity of the mushy layer.

The transport of solute takes the form (we use the Scheil equation to describe the mass transfer in a mush [17])

$$\frac{\partial}{\partial t}((1-\varphi)C_m) = 0, \quad a(t) < z < b(t), \quad (8)$$

where $C_m$ is the brine salinity (integration gives the Scheil formula known in metallurgy). This equation implies that the solid phase is nearly pure ice. Formula (8) is frequently applied by a number of investigators (see, among other, [15] and [17]). It is a good approximation for the impurity redistribution during the crystal growth for a wide range of experimental conditions (e.g. [18]). Within the mushy layer the local salinity of the liquid phase and the local temperature are related to one another through the phase diagram for sea ice [19]. In the range of salinities encountered here, this salinity-dependent freezing point is expressed by the linear phase diagram

$$T_m = -mC_m, \quad a(t) < z < b(t), \quad (9)$$

where $m$ is the liquidus slope.

The boundary conditions applied at the sea ice/mushy layer interface are [5,20]

$$\varphi = \varphi_a, \quad T_i = T_m, \quad z = a(t), \quad (10)$$

$$L_V(1-\varphi_a)\frac{da}{dt} = k_i\frac{\partial T_i}{\partial z} - [k_i\varphi_a + k_w(1-\varphi_a)]\frac{\partial T_m}{\partial z}, \quad z = a(t), \quad (11)$$

$$C_m(1-\varphi_a)\frac{da}{dt} = -D_w(1-\varphi_a)\frac{\partial C_m}{\partial z}, \quad z = a(t), \quad (12)$$

where $\varphi_a = \varphi_a(t)$ is the solid fraction at $z = a(t)$, $k_w$ and $D_w$ are the thermal conductivity and diffusion coefficient of the

pure water. The thermal properties of the mush are assumed to be volume-fraction-weighted averages of the properties of the individual phases so that $k_m(\varphi) = k_i\varphi + k_w(1-\varphi)$ (see, among others, [5,20–22]).

Further, we have the boundary conditions imposed at the interface between mushy layer and the relatively warm isothermal ocean ($T_w = \text{const}$)

$$\varphi = \varphi_b, \quad T_m = T_w, \quad z = b(t), \tag{13}$$

$$L_V\varphi_b\frac{db}{dt} = [k_i\varphi_b + k_w(1-\varphi_b)]\frac{\partial T_m}{\partial z}, \quad z = b(t), \tag{14}$$

where $\varphi_b$ is the solid fraction at $z = b(t)$, and $T_w$ is the constant temperature of the liquid (sea water) determined for $z \geqslant b(t)$. It must be emphasized that the mass balance condition at $z = b(t)$, analogous to the boundary condition (12), is absent within the framework of our model. This is due to the fact that some variations in the temperature gradient at $z = b(t)$ on the mush side of the interface (constant temperature in the ocean) leads to corresponding variations in the brine salinity gradient at $z = b(t)$ and, therefore, to variations in the mushy layer thickness in accordance with the criterion for constitutional supercooling (this condition holds for the mushy layer and its boundaries), which is

$$\frac{\partial T_m}{\partial z} = -m\frac{\partial C_m}{\partial z}.$$

Physically, a decrease in the temperature within the liquid boundary layer causes crystallization process, which is in progress until the local salinity attains its equilibrium value for a given temperature.

Integrating Eq. (8) and taking into account expressions (6), (9) and (13), we come to the solid phase distribution within the mushy layer (similar form of $\varphi$ is deduced by Wettlaufer et al. [16])

$$\varphi(z,t) = 1 + \frac{T_w(\varphi_b - 1)}{T_1(t) + zT_2(t)}. \tag{15}$$

Substitution of expressions (5), (6), (9) and (15) into the boundary conditions (10)–(15) gives

$$\varphi_a(t) = 1 + \frac{T_w(\varphi_b - 1)}{T_{at}(t) + C_1(t)a(t)}, \tag{16}$$

$$C_1(t) = \frac{L_V(1-\varphi_a)}{k_i}\frac{da}{dt} + [\varphi_a + K(1-\varphi_a)]T_2(t), \quad K = \frac{k_w}{k_i}, \tag{17}$$

$$T_{at}(t) + C_1(t)a(t) = T_w + T_2(t)(a(t) - b(t)), \tag{18}$$

$$[T_2(t)(b(t) - a(t)) - T_w](1-\varphi_a)\frac{da}{dt} = D_w(1-\varphi_a)T_2(t), \tag{19}$$

$$T_2(t) = \frac{L_V\varphi_b}{\Phi}\frac{db}{dt}, \quad \Phi = \Phi(\varphi_b) = k_i\varphi_b + k_w(1-\varphi_b), \tag{20}$$

$$T_1(t) = T_w - b(t)T_2(t). \tag{21}$$

As is seen from expression (16), if we suppose $\varphi_a = 1$, it immediately follows that $\varphi_b = 1$, that is, the mushy layer is entirely filled with the solid material (frontal model). In view of the fact that we seek an alternative solution ($\varphi_a \neq 1$), like factors, $1 - \varphi_a$, can be cancelled from both sides of (19).

Combining expressions (16), (18) and (20), we find the solid fraction at the ice/mushy layer interface in the form

$$\varphi_a(t) = 1 + \frac{T_w(\varphi_b - 1)}{T_w + \frac{L_V\varphi_b}{\Phi}\frac{db}{dt}(a(t) - b(t))}. \tag{22}$$

Eliminating $T_2(t)$ from expressions (19) and (20), we have

$$\left[(a(t) - b(t))\frac{L_V\varphi_b}{\Phi}\frac{db}{dt} + T_w\right]\frac{da}{dt} = -\frac{D_wL_V\varphi_b}{\Phi}\frac{db}{dt}. \tag{23}$$

Substituting $C_1(t)$ and $T_2(t)$ from expressions (17) and (20) into condition (18), eliminating $\varphi_a(t)$ by means of formula (22), we get the nonlinear differential equation containing functions $a(t)$ and $b(t)$:

$$L_VT_w(\varphi_b - 1)\left[(1-K)\frac{\varphi_b}{\Phi}\frac{db}{dt} - \frac{1}{k_i}\frac{da}{dt}\right]a(t) = \left(T_w - T_{at}(t) - \frac{L_V\varphi_b}{\Phi}b(t)\frac{db}{dt}\right)\left[(a(t) - b(t))\frac{L_V\varphi_b}{\Phi}\frac{db}{dt} + T_w\right]. \tag{24}$$

Expressions (23) and (24) represent the highly nonlinear differential system for $a(t)$ and $b(t)$. Let us consider three possible analytic solutions describing real solidification conditions. The first solution consists in the following. In view of the fact that the interfaces move relatively slowly [14,16], we arrive at the linear differential equation connecting $a(t)$ and $b(t)$ (neglecting the term proportional to $(da/dt)(db/dt)$ in Eq. (23)). Integrating this equation in view of the initial conditions $a(0) = b(0) = 0$, we get

$$a(t) = -\frac{D_wL_V\varphi_b}{T_w\Phi}b(t) \tag{25}$$

($a(t)/b(t) = 0.071$ for the physical parameters under consideration and $\varphi_b = 0.5$). We choose these initial conditions because a characteristic time of observations [14] is many times higher than a time of mushy layer initiation.

Further, substituting the term in square brackets from (23) into (24), taking into account (25), we come to the linear differential equation for $b^2(t)$:

$$\frac{I}{2}\frac{db^2}{dt} = T_w - T_{at}(t),$$

where

$$I = \frac{L_V\varphi_b}{\Phi}\left[1 - \frac{D_wL_V\varphi_b}{T_w\Phi}\left(\frac{L_VD_w}{k_iT_w} + 1 - K\right)(\varphi_b - 1)\right].$$

After integration of this equation ($b(0) = 0$), we find the mushy layer/liquid interface

$$b(t) = \sqrt{\frac{2}{I}\left(T_wt - \int_0^t T_{at}(\alpha)\,d\alpha\right)}. \tag{26}$$

Expression (26) shows that the interfaces $a(t)$ and $b(t)$, as would be expected, become self-similar [20] if the surface (atmospheric) temperature $T_{at}$ is constant. If the atmospheric temperature undergoes different time variations,

the interfaces $a(t)$ and $b(t)$ lie between two self-similar regimes, which correspond to the maximum ($T_{\max}$) and minimum ($T_{\min}$) ice surface temperatures measured in experiments. So, for example, for the mushy layer/ocean interface, we have

$$\sqrt{\frac{2}{I}(T_{\mathrm{w}}-T_{\max})t}\leqslant b(t)\leqslant\sqrt{\frac{2}{I}(T_{\mathrm{w}}-T_{\min})t}.$$

Thus, the nonlinear problem under consideration is solved analytically (explicit form of solutions is given by expressions (5), (6), (9), (15), (17), (20)–(22), (25), (26)). Let us especially emphasize that the solution depends on one free parameter $\varphi_b$ (this value cannot be found in the context of the theory under consideration). The solid fraction $\varphi_b$ must be found semi-empirically (when one of the functions found theoretically is compared with experiments). Then all of the rest functions will be completely known for any depths and times.

We have been interested to compare the mushy layer theory with the frontal analogue. If we formally put $\varphi_b = 1$ (the mushy layer is entirely filled with the sea ice), it is easy to see that expression (26) transforms to expression (4), $\varphi_{\mathrm{a}}(t)$ and $\varphi(z,t)\to 1$, $T_1(t)$ and $C_1(t)=T_2(t)$ become $T_{\mathrm{at}}(t)$ and $(T_{\mathrm{w}}-T_{\mathrm{at}}(t))/h(t)$, respectively. In other words, our explicit solutions for the mushy layer transform to their analogues for the planar front.

Fig. 2 demonstrates how the theory under consideration agrees with experimental data [14,16] for young sea ices. The free parameter $\varphi_b$ is chosen in such a manner that one of the functions found theoretically would approximate its experimental analogue (it is easily seen from Fig. 2 that all of the rest functions found theoretically are in a good agreement with observations for this value of $\varphi_b$). All of the curves plotted for two values of $\varphi_b$ essentially differ from the frontal solutions and properly describe the solidification dynamics of ice thickness and temperature fluctuations. The solid fraction at the sea ice/mushy layer interface as a function of time is shown in Fig. 3. An important point is that $\varphi_{\mathrm{a}}$ and $\varphi$ ($\varphi_b\leqslant\varphi\leqslant\varphi_{\mathrm{a}}$) undergo only insignificant time and spatial variations (a rapid growth of $\varphi$ occurs only at the early stages of the process, ~100 min, when a thin ice cover appears). Taking into account the latter and the fact that the temperature relaxation time is many times smaller than a characteristic time of the front motion, we conclude that Eq. (7) can be approximated by means of equation $\partial^2 T_{\mathrm{m}}(z,t)/\partial z^2=0$. Now, it is easily seen that the linear temperature profile (6) exactly satisfies to this equation and approximately describes the heat balance in the form of Eq. (7).

It is important to keep in mind that the sea ice/ocean interface in nature does not divide pure ice and freezing ocean, and divides the mushy layer with a high content of ice ($\varphi\sim 0.5$–$0.9$, Fig. 3) and sea water free of ice structures. The sea ice/mushy layer interface, $a(t)$, lags behind the mushy layer/ocean interface, $b(t)$, by virtue of the fact that the process of ice formation is hampered within the mushy layer with a high content of ice (all of the impurities rejected by the ice lattice are initially retained within the interstices of a layer of sea ice).

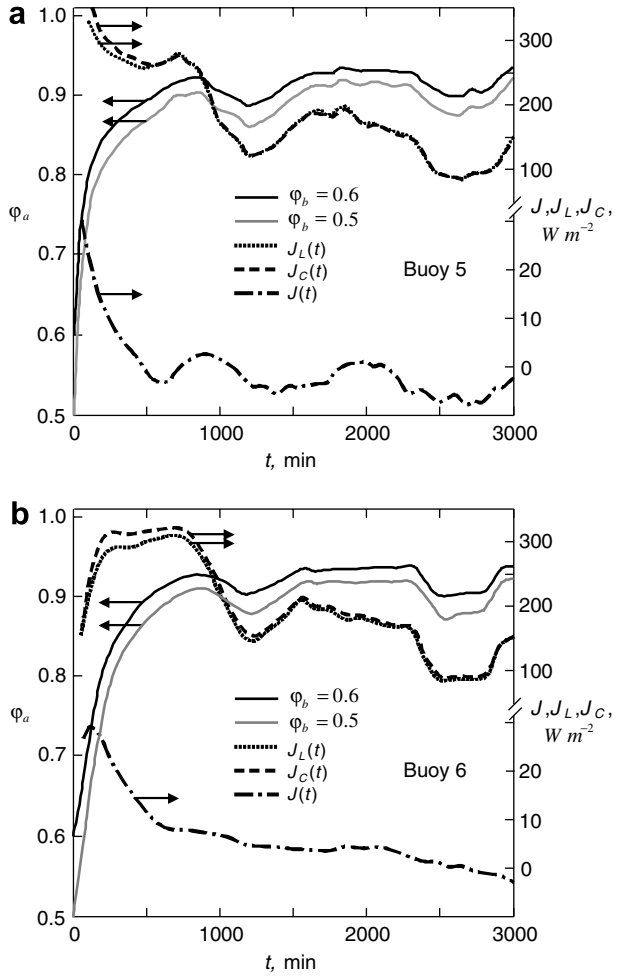


Fig. 3. Time series of the solid fraction $\varphi_{\mathrm{a}}$ (scale of values on the left) and heat fluxes (scale of values on the right) for (a) buoy 5 and (b) buoy 6. Heat fluxes are calculated for $\varphi_b = 0.5$ (buoy 5) and $\varphi_b = 0.6$ (buoy 6). Black circles designate experimental data [23].

Let us pay our attention to the conductive heat flux released to the atmosphere from the sea ice/atmosphere interface at $z = 0$. Within the framework of the model under consideration, this flux can be written in the form $J_{\mathrm{C}}(t) = k_{\mathrm{i}}C_1(t)$. This flux stems from the latent heat flux and other factors. Let us write down the mean latent heat flux as

$$J_{\mathrm{L}}(t)=\frac{L_V}{b(t)-a(t)}\int_{a(t)}^{b(t)}\varphi(z,t)\,\mathrm{d}z\left(\frac{\mathrm{d}b}{\mathrm{d}t}-\frac{\mathrm{d}a}{\mathrm{d}t}\right).$$

In view of insignificant rates of change of $a(t)$ with time (see also Fig. 2a and c), the term stemming from the motion of this boundary is omitted. Fig. 3 demonstrating time variations of the fluxes shows that $J_{\mathrm{C}}(t)$ and $J_{\mathrm{L}}(t)$ lie close to each other. The residual heat flux $J(t)=J_{\mathrm{C}}(t)-J_{\mathrm{L}}(t)$ (see Fig. 3), within the framework of the model under consideration, stems from the fact that the heat releases to the atmosphere. In order to explain the latter it is necessary to

say that the residual flux is significant only during initial stages of the process (Fig. 3 illustrates its dynamics hereafter, where the flux drops and oscillates in the vicinity of $J = 0$). In other words, the role of $J$ makes itself evident during essential variations in the solid fraction. It should be noted that the heat flux $J(t)$ decreases when the atmospheric temperature goes down and, as a consequence, when the mushy layer increases most rapidly (these instants of time are shown by slight crests of $b(t)$ in Fig. 2a and c). The total oceanic heat flux differs from the residual flux $J(t)$ because some additions (e.g., the turbulent oceanic heat flux at the underside of the ice, the solar radiation heat flux reflected from the ice cover, etc. may be mentioned) appear in nature. Some of these factors can be analyzed in the spirit of this paper. Let us emphasize in conclusion that the heat fluxes $J_C(t)$ or $J_L(t)$, obtained theoretically on the basis of experimental data, approximately represent the total heat flux per unit area lost during solidification of leads (as is seen, these fluxes are in a good agreement with field observations [23] on young sea ice dynamics).

Let us obtain the second analytic solution which describes the self-similar solidification from a cooled boundary of constant temperature [20]. Substituting the term in square brackets from (23) into (24), neglecting $da/dt$ in comparison with $db/dt$ and taking into account small temperature oscillations

$$|T_{at}(t)| \sim |T_w| \ll \frac{L_V \varphi_b}{\Phi} b(t) \frac{db}{dt}$$

(this case is frequently occurs in practice), we get

$$b(t) = Aa(t), \quad A = \sqrt{\frac{T_w(\varphi_b - 1)(1-K)\Phi}{D_w L_V \varphi_b}}. \tag{27}$$

Keeping in mind the strong inequality, from (23) we obtain

$$a(t) = \sqrt{\frac{2D_w}{A-1}}t. \tag{28}$$

Expressions (27) and (28) correspond to the case when the solidification boundaries are proportional to the square root of time and the regime under consideration is far from initial stages [20,24].

Let us pay our attention to the third analytic solution of Eqs. (23) and (24). Again, substituting the term in square brackets from (23) into (24), neglecting $da/dt$ in comparison with $db/dt$, we come to nonlinear differential equation of the form

$$\frac{T_w}{2D_w}(\varphi_b - 1)(1-K)a^2(t) - \frac{L_V \varphi_b}{2\Phi} b^2(t) + T_w t - \int_0^t T_{at}(\alpha)\,d\alpha = 0.$$

Taking into account $a \ll b$, we have the following expressions for the phase transition boundaries:

$$b(t) = \sqrt{\frac{2\Phi}{L_V \varphi_b}\left(T_w t - \int_0^t T_{at}(\alpha)\,d\alpha\right)}, \tag{29}$$

$$a(t) = -D_w \int_0^t \frac{(T_w - T_{at}(\alpha))\,d\alpha}{T_{at}(\alpha) b(\alpha)}. \tag{30}$$

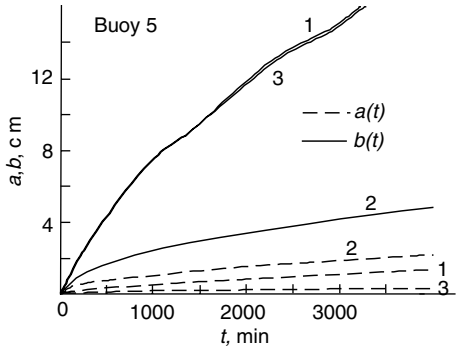


Fig. 4. Three analytic solutions for the mushy layer boundaries: 1 – (25) and (26), 2 – (27) and (28), 3 – (29) and (30). Numbers at the curves designate corresponding solutions.

Fig. 4 illustrates obtained solutions for different solidification conditions. Curves 1 and 3 practically coincide for the phase transition boundary $b(t)$ (also these curves are in a good agreement with experimental data, see Fig. 2) due to similar physical hypotheses taken into consideration above. Two solutions of $a(t)$ plotted for curves 1 and 3 show that the phase transition boundary $a(t)$ is practically frozen in comparison with $b(t)$. This means that the solidification domain (solid and mushy regions) can be considered as a mushy layer. This is due to the fact that solidification domains represent rather loose structures in natural conditions (see, among others, [23,25]).

## Acknowledgements

This work was made possible in part by Award No. REC-005 (EK-005-X1) of the US Civilian Research and Development Foundation for the Independent States of the Former Soviet Union (CRDF) and due to the financial support of grants Nos. 05-01-00240 (Russian Foundation for Basic Research) and MD-7106.2006.2 (President Grant).

## References

[1] I. Stefan, Uber einige Probleme der Theorie der Warmeleitung, Sitzber. Kais. Akad. Wiss. Wien, Math.-Naturw. Kl. 98 (11a) (1898) 437–438.
[2] H.S. Carslaw, J.C. Jaeger, Conduction of Heat in Solids, Oxford University Press, 1959.
[3] L.I. Rubinstein, The Stefan Problem, American Mathematical Society, 1969.
[4] R.L. Parker, Crystal Growth Mechanisms: Energetics, Kinetics and Transport, Solid State Physics, vol. 25, Academic Press, New York and London, 1970.
[5] Yu.A. Buyevich, D.V. Alexandrov, V.V. Mansurov, Macrokinetics of Crystallization, Begell House, New York and Wallingford, 2001.
[6] J. Crank, Free and Moving Boundary Problems, Clarendon Press, Oxford, 1984.
[7] G.P. Ivantsov, The diffusion supercooling in crystallization of a binary mixture, Dokl. Acad. Nauk SSSR 81 (2) (1947) 179–182.
[8] W.A. Tiller, K.A. Jackson, J.M. Rutter, B. Chalmers, The redistribution of solute atoms during the solidification of metals, Acta Metall. 1 (4) (1953) 428–437.

[9] W.A. Tiller, J.M. Rutter, The effect of growth conditions upon the solidification of a binary alloy, Can. J. Phys. 34 (1956) 96–121.
[10] W.W. Mullins, R.F. Sekerka, Stability of a planar interface during solidification of a dilute binary alloy, J. Appl. Phys. 35 (1964) 444–451.
[11] V.T. Borisov, Crystallization of binary mixture without loss of stability, Dokl. Acad. Nauk SSSR 136 (3) (1961) 516–519.
[12] R.N. Hills, D.E. Loper, P.H. Roberts, A thermodynamically consistent model of a mushy zone, Q. J. Appl. Math. 36 (1983) 505–539.
[13] A.C. Fowler, The formation of freckles in binary alloys, IMA J. Appl. Math. 35 (1985) 159–174.
[14] J. Morison, M. McPhee, R. Muench, et al., The LeadEx experiment, Eos. Trans. AGU 74 (1993) 393–397.
[15] E. Scheil, Bemerkungen zur schichtkiistallbildung, Z. Metall. 34 (1942) 70–72.
[16] J.S. Wettlaufer, M.G. Worster, H.E. Huppert, Solidification of leads: theory, experiment, and field observations, J. Geophys. Res. 105 (2000) 1123–1134.
[17] R.C. Kerr, A.W. Woods, M.G. Worster, H.E. Huppert, Solidification of an alloy cooled from above. Part 1. Equilibrium growth, J. Fluid Mech. 216 (1990) 323–342.
[18] M.C. Flemings, Solidification Processing, McGraw-Hill Book Company, New York, 1974.
[19] W.F. Weeks, Growth conditions and the structure and properties of sea ice, in: M. Leppäranta (Ed.), Physics of Ice-Covered Seas, University of Helsinki Press, Helsinki, 1998, pp. 25–104.
[20] M.G. Worster, Solidification of an alloy from a cooled boundary, J. Fluid Mech. 167 (1986) 481–501.
[21] G.K. Batchelor, Transport properties of two-phase materials with random structure, Ann. Rev. Fluid Mech. 6 (1974) 227–255.
[22] Yu.A. Buyevich, D.V. Alexandrov, Heat Transfer in Dispersions, Begell House Inc., New York–Wallingford, 2005.
[23] D.K. Perovich, J.A. Richter-Menge, Ice growth and solar heating in springtime leads, J. Geophys. Res. 105 (2000) 6541–6548.
[24] D.V. Alexandrov, A.P. Malygin, Self-similar solidification of an alloy from a cooled boundary, Int. J. Heat Mass Transfer 49 (2006) 763–769.
[25] A.J. Gow, D.A. Meese, D.K. Perovich, W.B. Tucker III, The anatomy of a freezing lead, J. Geophys. Res. 95 (1990) 18.221–18.232.